# Dynamic Path-Protected Service Provisioning in Optical Transport Networks with a Limited Number of Add/Drop Ports and Transmitter Tunability

Gangxiang Shen, *Member, IEEE,* and Wayne D. Grover, *Fellow, IEEE*

***Abstract*— We consider path-based survivable service provisioning in transparent optical networks with the constraints of wavelength continuity and a limited number of add/drop ports at each OXC node in the presence of limited tunability of transmitters. We develop simple but valid analytical models to estimate the effects of number of add/drop ports and transmitter tunability on survivable service provisioning performance. We propose effective algorithms for the assignments of wavelength resources and add/drop ports for each survivable connection service and conduct simulations to evaluate the impacts of number of add/drop ports and transmitter tunability on path-based survivable service provisioning and further to examine the validity of the analytical models. It is found that a certain system add/drop ratio is required at each node so as to eliminate the blocking due to the lack of free add/drop ports. A network with a higher density requires a larger relative number of add/drop ports (i.e., add/drop ratio) for a given overall blocking objective. A network with a higher density benefits more in blocking from transmitter tunability. Finally, the analytical models are verified to be able to qualitatively predict the trends and effects of all the related constraints on the performance of survivable service provisioning.**

***Index Terms*— Network survivability, shared backup path protection, wavelength continuity, lightpath service provisioning, transmitter tunability, limited add/drop ports.**

## I. Introduction

PATH-BASED optical survivable service provisioning can be implemented in a fashion of either traditional 1:1 or more advanced shared backup path protection (SBPP) approaches [1]–[8]. Most recent studies on SBPP-based survivable service provisioning were focused on MPLS networks or optical networks with full wavelength conversion, in which the information of working and protection capacity is maintained in an aggregate fashion [3]–[5], [7], [8]. Having wavelength conversion everywhere in a network simplifies operation, but the cost of wavelength conversion remains high, so dealing with the constraint of wavelength continuity is significant for dynamic survivable lightpath service provisioning. For this type of network, the approach based on the aggregate routing information is not adequate, but a per-connection model is required to distinguish the status of each individual wavelength channel [6], [9]. Specifically, the information on whether a given wavelength channel is free or occupied, a list of protection paths that share a common protection channel, and the wavelength index of a channel, etc., should be maintained.

Relatively little research however has been considered for SBPP service provisioning in the optical network with the constraint of wavelength continuity. In [10], the schemes termed *backup multiplexing* and *primary-backup multiplexing* were investigated based on fully maintained per-flow (or per-connection) routing information. Two sub-cases were studied for backup multiplexing, which involved the constraint of whether or not a pair of working and protection lightpaths should use an identical wavelength. In [11], SBPP-based protection mechanisms were implemented in optical networks with partial wavelength conversion capability, in which *conversion free primary routing* (CFPR) and *converter multiplexing* techniques were explored. Recently, a segment-based protection scheme was also developed for optical networks with partial wavelength conversion [12].

Moreover, most of the previous research assumed a full number add/drop ports were deployed at each OXC node, and transmitters in the add/drop ports had full tunability to be tuned to any wavelength in a fibre spectrum. However, a full number of add/drop ports may not be common in realistic optical transport networks as it is not economic owing to the fact that a high percentage of lightpaths incident on a node only traverse the node. Also, not to mention whether a tunable transmitter can cover a full spectrum of an optical transmission system, a transmitter with wider tunability is generally more expensive than a fixed transmitter or a transmitter with a smaller tuning range. Thus, for lightpath service provisioning, it is also significant to consider the constraints of a limited number of add/drop ports and limited transmitter tunability.

Earlier investigation was performed to evaluate the impact of number of add/drop ports and transmitter tunability in a wavelength-continuous optical transport network. A preliminary simulation study [13] was first conducted and then an analytical model [14] was developed based on the fixed point relaxation theory to compute lightpath blocking probability. It was found that a limited number of add/drop ports and limited transmitter tunability can achieve a performance close to that of a full number add/drop ports and full transmitter tunability. However, the above research only considered non-protected services. For path-based survivable services, the problem is much more challenging as more constraints should be taken

Manuscript received August 9, 2006; revised April 29, 2007.

G. Shen is with the ARC Special Research Center for Ultra-Broadband Information Networks, the Department of Electrical and Computer Engineering, University of Melbourne, Melbourne, VIC, 3010 Australia (e-mail: g.shen@ee.unimelb.edu.au).

W. D. Grover is with TRLabs, Department of Electrical and Computer Engineering, University of Alberta, Alberta, Canada (email: grover@trlabs.ca).

Digital Object Identifier 10.1109/JSAC-OCN.2007.027806.

into account. First, spare capacity sharing among wavelength-continuous protection lightpaths should be considered for efficient capacity utilization. Second, whether a pair of working and protection lightpaths that makes up a survivable service should use an identical wavelength or different wavelengths depends on the transmitter tunability at the source node of a survivable connection.

Fig. 1 illustrates how transmitter tunability can constrain the wavelengths used by a pair of working and protection lightpaths. If the transmitter is not tunable as shown in Fig. 1(a), the working and protection lightpaths must use an identical wavelength. That is, the two lightpaths must be established in a common wavelength plane, e.g., wavelength plane 1. However, if the transmitter is fully tunable as shown in Fig. 1(b), the two lightpaths can be independently established in different wavelength planes, e.g., wavelength 1 and wavelength $w$, respectively. As an intermediate case, if the transmitter can only be partially tunable, the two lightpaths can be established in different wavelength planes, but the two planes must be close enough. Specifically, if the wavelength range that a partially tunable transmitter covers is $d$ (smaller than $w$) wavelengths, a pair of working and protection lightpaths can only be established in the wavelength planes indexed from 1 to $d+1$ as shown in Fig. 1(c).[1]

For survivable lightpath service provisioning, the effect of transmitter tunability was evaluated in [10], which compared two extreme cases: (1) fixed transmitter, and (2) fully tunable transmitter. While it is interesting to see that full transmitter tunability could improve blocking performance, a more general research is useful to consider how a limited tuning capability can improve the performance of path-based survivable service provisioning. Also, the study in [10] ignored the constraint of possible shortage of free add/drop port at OXC nodes by assuming a full number of add/drop ports (transceivers) are always available at each OXC node.

The present study aims to evaluate the performance of a path-based survivable lightpath service provisioning with the constraints of (1) limited number of add/drop ports at each OXC, (2) limited transmitter tunability, and (3) wavelength continuity of lightpath. We first develop analytical models considering the effects of transmitter tunability and limited number of add/drop ports. Then for online service provisioning, we propose an effective joint add/drop port and wavelength assignment algorithm. The algorithm will be used for simulation studies, but it is also eligible to the implementation of real optical transport networks. The simulation results are used to verify the effectiveness of the analytical models. The research also considers other aspects that may affect the service provisioning performance. These include (1) network density (nodal degree), (2) spare capacity sharing efficiency, (3) traffic intensity, and (4) the number of wavelengths on each link, etc.

As a limitation, this study ignores the impact of optical transparent reach limits [15] by assuming no 3R regeneration is required on the way of long-distance lightpaths. More practical (but complicated) investigation could be conducted to take such a constraint into account. Nonetheless, we believe that the methodology and output in the current research are also applicable to the study considering transparent reach limits.

[1]In this example, because the transmitter's central wavelength is assumed to be fixed on the spectrum boundary, its upper half tuning range is truncated. Suppose no truncation, a transmitter whose central wavelength is in the middle of a spectrum shall have a complete $(2d+1)$-wavelength coverage, including an upper $d$-wavelength range, a lower $d$-wavelength range, and the central wavelength itself.

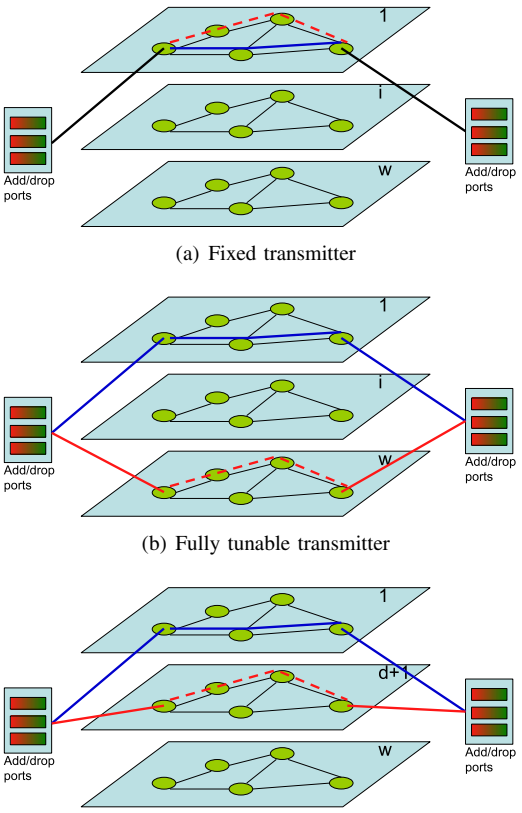


(a) Fixed transmitter

(b) Fully tunable transmitter

(c) Partially tunable transmitter (tuning degree $d$)

Fig. 1. Add/drop port sharing between working and protection lightpaths.

Also, an important point before proceeding is to emphasize that *tunability* is not the same as *wavelength conversion*. Such confusion may arise but the clearest way to point out the difference here is that in the networks we consider, there is *never any wavelength conversion*. These are transparent optical networks using entirely transparent OXCs without any wavelength conversion capability (except of course to transduce add/drop payload signals at their network entry or egress points). Thus in our context a wavelength must be assigned to a service path at its originating node, but thereafter whether launched from a fixed or tunable transmitter, the wavelength is never converted or changed enroute and the signal never leaves the optical domain until reaching its destination node.

## II. Generic Analytical Models for Path-Based Service Provisioning

We present generic analytical models for the qualitative study of path-based survivable service provisioning. Although simple, the models are expected to provide a valid performance prediction for both simple 1:1 service provisioning and more efficient SBPP service provisioning. The models are developed based on the assumption of link-independent

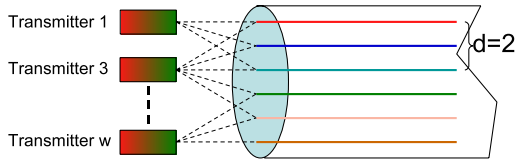


Fig. 2. Tuning range of partially tunable transmitter.

traffic model [16] and the portion of link capacity blocking is extended from the model in [17], which however does not consider network survivability. Following are the common terms that are used in the models:

$M$, $N$: numbers of network links and nodes, respectively.

$w$: number of wavelengths on each link. We assume there is the same number of wavelengths on each link.

$\rho$: average wavelength utilization on each link (in short, link utilization). Under the assumption of independent link traffic model, the average wavelength utilization on each link is assumed to be the same and independent of link index and wavelength index.[2]

$H_w$, $H_p$: average hop lengths of working and protection paths, respectively.

$\alpha$: spare capacity sharing coefficient. When a pair of working and protection lightpaths is established, the working lightpath always fully occupies an assigned wavelength unit, while the protection lightpath may share an assigned wavelength unit with other protection lightpaths under the SBPP scheme. Thus, only a fraction of wavelength unit is essentially used by the protection lightpath. For example, if a protection capacity unit is shared by $L$ protection lightpaths, then the coefficient is equal to $1/L$. To reflect this fractional utilization, we introduce this spare capacity sharing coefficient to the models. Specifically, for SBPP, $\alpha$ is within the range of (0, 1.0), and the smaller $\alpha$ is, the more efficient the SBPP scheme is, and vice versa. As two special cases, $\alpha$ can be 0, which corresponds to the case of without protection, and $\alpha$ can be 1.0, which corresponds to the case of 1:1 survivable service provisioning.

$d$: *tuning degree* of a transmitter. Following the definition of limited-range wavelength conversion degree in [18], given a tuning degree $d$, a transmitter at a central wavelength $\lambda$ can be tuned within a tuning range of $[\lambda - d, \lambda + d]$. Note that if $\lambda - d$ is smaller than wavelength index 1 (the lower boundary index of a spectrum), it is truncated as index 1; in the other extreme, if $\lambda + d$ is larger than wavelength index $w$ (the upper boundary index of a spectrum), it is truncated as index $w$. Thus, transmitters whose central wavelengths are close to the upper or lower boundary of a wavelength spectrum generally cover smaller wavelength-tuning ranges than those of the transmitters that are in the *middle* of the wavelength spectrum. Due to the non-uniformity of transmitter tuning range, a term called *average tuning range* $\bar{r}$ will be defined later. Fig. 2 illustrates how the tuning range changes with the location of central wavelength within a wavelength spectrum. Given $d = 2$, because transmitter 1 and transmitter $w$ have central wavelengths respectively on the spectrum boundaries, they have a tuning range of three wavelengths only. In contrast, because transmitter 3 has a central wavelength indexed at 3, it covers a tuning range of up to five wavelengths.

An efficient strategy of central wavelength allocation for each transmitter can be employed to avoid the truncation of tuning range when the central wavelength of a transmitter is located on the boundary of a wavelength spectrum. That is, whenever tuning range (lower or upper) truncation occurs, we replace the transmitter with a new transmitter whose central wavelength is on $d+1$ (for lower boundary truncation) or $w-d$ (for upper boundary truncation). As such, the overall tuning range of each transmitter can be ensured to be either $2d+1$ when $2d+1 < w$, or $w$ when $2d+1 \geq w$. We do have conducted simulation studies based on this type of central wavelength allocation strategy. Similar results and observations were obtained to those reported in the paper with the performance of the former (very) marginally better than the latter. Here for the purpose of central wavelength consistency between the tunable and fixed transmitter study cases, we adopt the truncating strategy. However, the developed methodology in this study is general enough to be applicable to the case without truncation.

### *A. Analytical Models Evaluating the Impact of Transmitter Tunability*

To evaluate the impact of transmitter tunability, we assume that there are sufficient add/drop ports deployed at each node so as to isolate the impact from a limited number of add/drop ports. Under this assumption, the analytical model for the service blocking probability of the fixed transmitter case is as follows:

$$\begin{aligned} P_b &= (1-(1-\rho)^{H_w}(1-\alpha\rho)^{H_p})^w \\ &= (1-((1-\rho)(1-\alpha\rho))^H)^w \quad \text{if} \quad H_w \simeq H_p = H. \end{aligned} \tag{1}$$

As shown in Fig. 1(a), because there is no wavelength tunability on each transmitter, the working and protection lightpaths must use the same wavelength on their routes, i.e., they must be established on a common wavelength plane. Recall that $\alpha$ indicates the spare capacity sharing efficiency of protection lightpaths. Thus, the term $\alpha\rho$ represents the average wavelength capacity used by a protection lightpath on each link. The term $(1-\rho)^{H_w}(1-\alpha\rho)^{H_p}$ represents the probability of successfully establishing a pair of working and protection lightpaths in a common wavelength plane. The term $(1-(1-\rho)^{H_w}(1-\alpha\rho)^{H_p})^w$ therefore represents the probability that a pair of working and protection lightpaths cannot be established on any one of $w$ wavelength planes. Moreover, if an approximation $H_w \simeq H_p = H$ is made, then the overall blocking probability $P_b$ can be simplified as $(1-((1-\rho)(1-\alpha\rho))^H)^w$.

Similarly, with full wavelength tunability, the blocking probability can be computed as:

$$\begin{aligned} P_b &= 1-(1-(1-(1-\rho)^{H_w})^w)(1-(1-(1-\alpha\rho)^{H_p})^w) \\ &= 1-(1-(1-(1-\rho)^H)^w)(1-(1-(1-\alpha\rho)^H)^w) \\ &\quad \text{if} \quad H_w \simeq H_p = H. \end{aligned} \tag{2}$$

[2]It is known that analytical models based on average link utilization may be optimistic regarding blocking performance because they do not reflect link-to-link state correlations that may develop under actual traffic patterns.

TABLE I
MAPPING BETWEEN $d$ AND $\bar{r}$ WHEN $w = 8$

| $d$ | 0 | 1 | 2 | 3 | 4 | 5 | 6 | 7 | 8 |
|---|---|---|---|---|---|---|---|---|---|
| $\bar{r}$ | 1 | 2.75 | 4.25 | 5.50 | 6.50 | 7.25 | 7.75 | 8.0 | 8.0 |

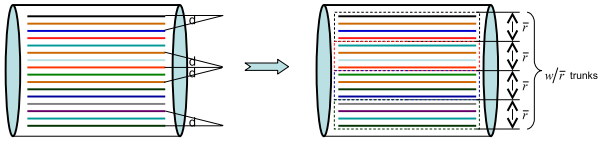


Fig. 3. Approximate transformation from tuning degree $d$ to multiple $w/\bar{r}$ fully tunable small trunks.

In this case, the working and protection lightpaths are not required to be established in a common wavelength plane. They can be set up independently in different wavelength planes as shown in Fig. 1(b). The term $1-(1-(1-\rho)^{H_w})^w$ denotes the success probability that a working lightpath can be established on at least one of $w$ wavelength planes. For the protection lightpath, a similar computation can be made except that $\rho$ is replaced by $\alpha\rho$.

Next, we consider the partially tunable case. Given a tuning degree $d$ and the number of wavelengths on each link $w$, the average tuning range $\bar{r}$ can be computed as:

$$\bar{r} = \frac{\sum_{i=1}^{w}(\min(i+d,w) - \max(i-d,1)+1)}{w}. \quad (3)$$

The equation averages wavelength tuning ranges over the scenarios of different transmitter central wavelengths. The term $\min(i+d,w) - \max(i-d,1)+1$ computes a tuning range when the central wavelength of a transmitter is $i$. Table I shows some data of $d$ and $\bar{r}$ when $w = 8$.

To model the partially tunable case, we first make an approximate transformation for a $w$-wavelength spectrum. This transformation is similar to the one modeling limited-range wavelength conversion in [19]. Specifically, the wavelength spectrum with a partially tuning degree is approximately transformed into a spectrum containing several parallel fully tunable smaller trunks, with each trunk consisting of $\bar{r}$ channels. Fig. 3 illustrates such an approximation. A protection service can be provisioned within each of such trunks, with the working and protection paths established on different wavelengths. Nonetheless, it is not allowed to provision a survivable service with a working lightpath established within one trunk while a protection lightpath within another trunk, as the transmitter tunability is approximated to cover only the wavelengths within a common trunk.

Based on the transformation, we can compute the probability that a pair of working and protection paths fail to be established within a $\bar{r}$-channel trunk as follows:

$$\begin{aligned} P_b^{trunk} &= 1-(1-(1-(1-\rho)^{H_w})^{\bar{r}})(1-(1-(1-\alpha\rho)^{H_p})^{\bar{r}}) \\ &= 1-(1-(1-(1-\rho)^{H})^{\bar{r}})(1-(1-(1-\alpha\rho)^{H})^{\bar{r}}) \\ &\quad \text{if} \quad H_w \simeq H_p = H. \end{aligned} \quad (4)$$

The overall blocking probability for the partially tunable transmitter case is the probability that all the contained trunks fail to establish a pair of working and protection lightpaths. Thus,

$$\begin{aligned} P_b &= (P_b^{trunk})^{w/\bar{r}} \\ &= (1-(1-(1-(1-\rho)^{H})^{\bar{r}})(1-(1-(1-\alpha\rho)^{H})^{\bar{r}}))^{w/\bar{r}}. \end{aligned} \quad (5)$$

Here $w/\bar{r}$ is the number of $\bar{r}$-channel trunks in a $w$-wavelength spectrum. Note only for the analytical purpose, we allow $\bar{r}$ and $w/\bar{r}$ to be real values.

### B. Analysis of Add/Drop Ratios

Two types of add/drop ratios can be defined. One is *system add/drop ratio*, and the other is *traffic add/drop ratio*. System add/drop ratio is system hardware-oriented to represent the percentage of add/drop ports actually deployed at a node related to the total number of wavelengths incident to the node, which is defined as:

$$\gamma_s = T_s/(d_n w). \quad (6)$$

$T_s$ is the total number of system add/drop ports deployed at each node, $d_n$ is an average nodal degree, and thus $d_n w$ is the total number of wavelengths on average incident to the node.

Corresponding to system add/drop ratio, traffic add/drop ratio is defined as a ratio of actual lightpath traffic added/dropped at a node to the total lightpath traffic incident to the node:

$$\gamma_t = T_t/(d_n w \rho). \quad (7)$$

$T_t$ is the total number of lightpaths added/dropped at a node, and $d_n w\rho$ is the total number of wavelengths that are carrying *active* lightpaths on all the links incident to the node.

Mathematically, these two ratios are bound by the Erlang B formula. Specifically, to achieve a certain level of add/drop port blocking probability $P_{ad}$ (due to the lack of free add/drop ports), the two add/drop ratios hold a relationship as Erlang $B(\gamma_s d_n w, \gamma_t d_n w\rho) \leq P_{ad}$. Given $d_n = 3$, $w = 16$, and $P_{ad} \leq 0.1\%$, Fig. 4 shows curves between these two add/drop ratios under various link utilizations $\rho$. Clearly, from the figure, we can see that although these two add/drop ratios are bound by the Erlang B formula, they hold an approximately linear relationship. With the increase of link utilization, the slopes of the lines increase as well. Fig. 5 shows a relationship of the slopes of the lines in Fig. 4 versus link utilization $\rho$. Again, it is interesting to see that they hold an approximately linear relationship and the slope of the line is about 1.17. Based on these lines, given one add/drop ratio we can find the value of the other add/drop ratio. For example, assume a link utilization $\rho = 0.7$. Based on Fig. 5, we can find the corresponding slope of the line between the two add/drop ratios is 0.95. Now if traffic add/drop ratio is 0.6, based on the curve ($\rho = 0.7$) in Fig. 4, we can find a required system add/drop ratio 0.72, which ensures an add/drop port blocking probability $P_{ad} \leq 0.1\%$.

In addition to (7), we can use other intuitive terms to define the traffic add/drop ratio. These terms are related to practical traffic parameters such as hop lengths of working and protection lightpaths, spare capacity sharing efficiency of protection

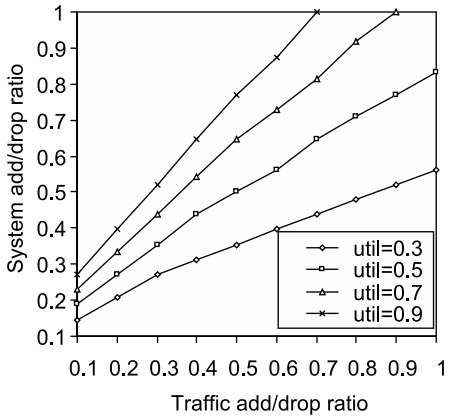


Fig. 4. Traffic add/drop ratio versus system add/drop ratio. Number of wavelengths $w = 16$, required add/drop port blocking probability $P_{ad} \leq 0.001$, and average nodal degree $d_n = 3$.

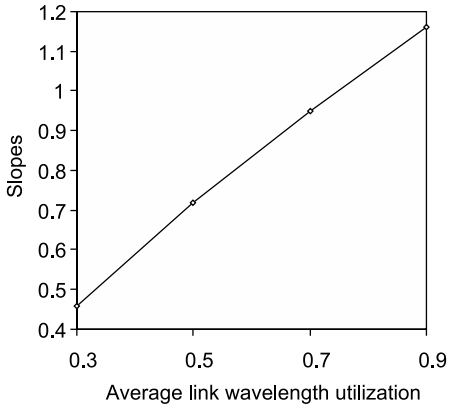


Fig. 5. The slope change of the lines in Fig. 4 with the increase of link utilization $\rho$.

lightpaths, etc. Recall that $H_w$ and $H_p$ represents the number of hops traversed by working and protection lightpaths, respectively. Thus, the term $H_w + \alpha H_p$ represents how many channel (capacity) hops on average consumed (traversed) by each survivable connection. Because each channel hop occupies a pair of switch ports at the two ends of the channel link, a survivable connection consumes a total of $2(H_w + \alpha H_p)$ switch ports, among which two ports (source and destination ports of the survivable connection) are add/drop ports, while all the other ports are traversing ports. Thus, we can define traffic add/drop ratio as

$$\gamma_t = 1/(H_w + \alpha H_p), \tag{8}$$

which is the ratio of the two source and destination add/drop ports to the total number of ports used by each survivable connection. Mathematically, definitions (7) and (8) are equivalent and we can derive them from each other.

Based on (8), it is easy to see that the more channel hops a survivable connection traverses and/or the larger term $\alpha$ (i.e., a less efficient SBPP scheme) is, the lower traffic add/drop ratio will be. These are all explainable. Longer lightpaths generally traverse more intermediate OXC nodes. Thus, relatively fewer add/drop ports are required. Also, more efficient spare capacity sharing (a smaller $\alpha$) enables to establish more survivable connections within a network, which requires more add/drop ports at source and destination nodes.

Based on (8), we also particularly consider two special topologies, i.e., a *ring* and a *complete mesh*, under the assumption of a *uniform* traffic demand distribution. Under a ring, SBPP shows a 100% spare capacity redundancy, which implies $H_w = \alpha H_p$. Thus, equation (8) can be derived to

$$\gamma_t = 1/(2H_w). \tag{9}$$

For an $N$-node ring, it is easy to find the average hop length of working lightpaths $H_w$ (based on the shortest path routing). We then substitute $H_w$ into (9) to derive traffic add/drop ratio as

$$\gamma_t = \begin{cases} \frac{2}{N+1} & \text{if } N = \text{odd} \\ \frac{2(N-1)}{N^2} & \text{if } N = \text{even.} \end{cases} \tag{10}$$

Based on (10), we can see that traffic add/drop ratio approaches zero when the number of network nodes $N$ increases to infinity. This is explainable because more lightpaths traverse OXC nodes with the increase of a ring size.

As the counterpart of a ring, a complete mesh network has a nodal degree $d_n = N - 1$ universally on each node. Under SBPP, each link can be efficiently shared by up to $2(d_n - 1)$ two-hop protection paths, which corresponds to $\alpha = 1/(2(d_n - 1))$. Also, a complete mesh network has $H_w = 1$ and $H_p = 2$. Thus, the corresponding traffic add/drop ratio is

$$\gamma_t = 1/(H_w + \alpha H_p) = 1/(1 + 1/(d_n - 1)) = (N-2)/N - 1). \tag{11}$$

Here term $1/(d_n - 1)$ is the lower bound on spare capacity redundancy of SBPP under a complete mesh network [20]. Obviously, traffic add/drop ratio $\gamma_t$ approaches one when the number of nodes $N$ increases to infinity. This is also explainable since in a complete mesh network, nodes tend to communicate via direct links and moreover there is a small sharing coefficient $\alpha$.

In summary, under SBPP a ring and a complete mesh networks respectively serve as lower and upper bounds on traffic add/drop ratios ranging from 0 to 1.0, and between them, traffic add/drop ratio increases with the decrease of average hop lengths of working and protection lightpaths, or, given the same number of nodes $N$, with the increase of average network nodal degree $d_n$.

Similar analyses can be performed for the protection cases of *without protection* and 1:1. Under a ring, the case of without protection has a traffic add/drop ratio equal to (10) divided by 2. The case of 1:1 has a traffic add/drop ratio $1/N$, as $\alpha = 1.0$ and a pair of working and protection lightpaths always forms a complete ring, i.e., $H_w + \alpha H_p = N$. In contrast, under a complete mesh network, because $H_w = 1$ and $H_p = 2$, the case of without protection has a traffic add/drop ratio $\gamma_t = 1/H_w = 1.0$ and the case of 1:1 has a traffic add/drop ratio $\gamma_t = 1/(H_w + H_p) = 1/3$.

For a generic network topology (not a ring or a complete mesh), traffic add/drop ratio can be generally derived as

$$\gamma_t = S/(C_w + C_p), \tag{12}$$

where $C_w$ and $C_p$ are the total amounts of used working and protection capacity, respectively, and $S$ is the total number

of survivable connections being served in a network. Thus, $(C_w+C_p)/S$ means the total amount of capacity used by each survivable connection. Meanwhile, in (8), we have defined $H_w + \alpha H_p$ as the total amount of capacity used by each survivable connection. Thus, the two terms are equivalent, and $(C_w+C_p)/S$ can replace $H_w+\alpha H_p$ in (8) to compute traffic add/drop ratio as (12).

From (12) it is easy to see that if a smaller amount of total capacity can serve the same number of connections, or the same amount of total capacity can serve a larger number of connections, traffic add/drop ratio is larger. Specifically for SBPP and 1:1, given the same demand matrix, SBPP shows a larger traffic add/drop ratio than that of 1:1, because SBPP is generally more efficient in spare capacity sharing than 1:1, and thus requires a smaller amount of total capacity $C_w+C_p$.

### C. Analytical Model Evaluating Impact of Number of Add/Drop Ports

Rather than a full number of add/drop ports as before, in this section, we evaluate the impact of number of add/drop ports on survivable lightpath service provisioning by assuming that there are a limited number of add/drop ports on each node. In order to isolate the impact from the transmitter tunability, we also assume that the transmitter on each add/drop port is fully tunable.[3]

Assume that there are $T_s$ add/drop ports deployed at each source and destination node. By taking into account the availability of free add/drop ports, the blocking probability of path-based survivable service provisioning is

$$P_b = 1 - (1 - B_s(T_s))(1 - P_b^{capacity})(1 - B_d(T_s)). \quad (13)$$

Here $P_b^{capacity}$ is the blocking probability due to limited link capacity, which is computed by (2). Given utilization of each add/drop port $\rho_{ad}$, the probability that $T_s$ add/drop ports are all occupied is $B(T_s) = \rho_{ad}^{T_s}$. Thus, $1 - B_s(T_s)$ and $1 - B_d(T_s)$ are probabilities of free add/drop ports available at the source and destination nodes respectively. Substituting (2) for $P_b^{capacity}$, we can get an overall blocking probability under the constraint of limited number of add/drop ports as:

$$P_b = 1-(1-\rho_{ad}^{T_s})^2(1-(1-(1-\rho)^H)^w)(1-(1-(1-\alpha\rho)^H)^w). \quad (14)$$

To compute (14), we need to know $\rho_{ad}$, which can be derived as

$$\rho_{ad} = \gamma_t w \rho d_n / T_s = (\gamma_t/\gamma_s)\rho. \quad (15)$$

The ratio $\gamma_t/\gamma_s$ is just the reciprocal of the slope of a line shown in Fig. 4. For example, when link utilization $\rho$ is 0.3, the slope of the line in Fig. 4 is 0.46, which yields an equation $\rho_{ad} = \rho/0.46 = 2.17\rho$.

## III. Results of Analytical Models

Based on the above analytical models, we make preliminary analyses on the impacts of transmitter tunability and number of add/drop ports on path-based survivable service provisioning.

[3]In the context of limited number of add/drop ports, it is feasible to develop analytical models for the other tunability cases, namely, fixed and partially tunable; however, due to complexity, we will use simulations for the study.

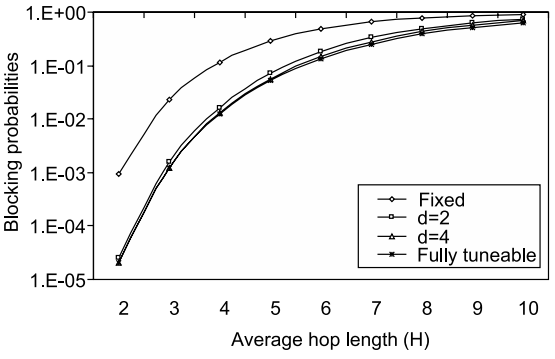


(a)

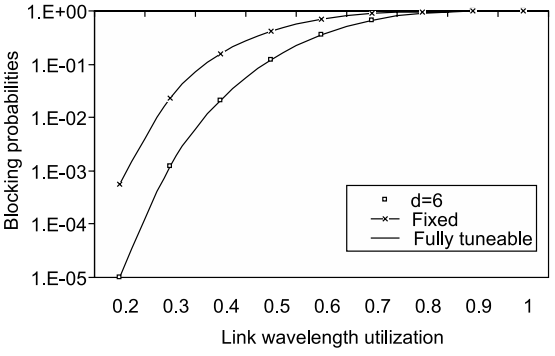


(b)

Fig. 6. Blocking performance versus (a) average hop length $H$ and (b) link utilization $\rho$. The number of wavelengths per link $w = 16$ and spare capacity sharing coefficient $\alpha = 0.5$.

Other impact factors such as network density, number of wavelengths on each link, spare capacity sharing efficiency, and traffic load intensity are also considered.

### A. Impact of Transmitter Tunability

Assuming link utilization $\rho$ is 0.3, Fig. 6(a) depicts how the service blocking probability changes with the transmitter tunability with the increase of average path hop length $H$ for the case of SBPP $(\alpha = 0.5)$. Following observations can be made:

First, it can be seen that a network with partially tunable transmitters can achieve a performance close to that of a network with fully tunable transmitters. Fig. 6(a) shows that a tuning degree $d = 4$ can achieve a performance close to that of fully tunable transmitter with $d = 16$. Second, with the increase of hop length $H$, the blocking probability increases as well. This is because it is more difficult to find a wavelength-continuous lightpath on a longer route. Finally, at a shorter hop length, it seems that full transmitter tunability can bring more performance improvement over the fixed transmitter case, which means that a network with higher network density generally benefits more from transmitter tunability. Similar observations were also found in our study for a 1:1 protected network $(\alpha = 1.0)$.

Under different link utilization, or, network traffic load, the effect of transmitter tunability was also studied to be shown in Fig. 6(b). By fixing average hop length $H = 3$ and number of wavelengths per link $w = 16$, we see that under lower link utilization, transmitter tunability can yield more performance

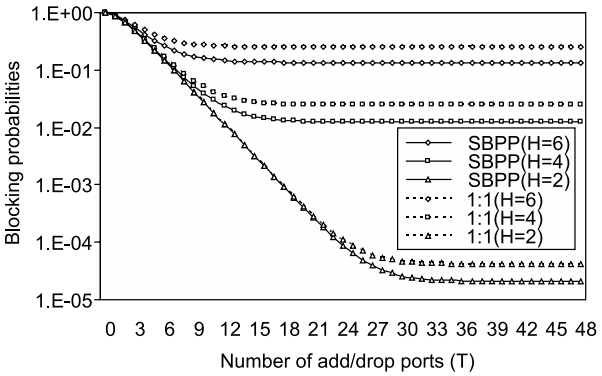


Fig. 7. The impact of limited number of add/drop ports varying with hop length $H$. Average link wavelength utilization $\rho = 0.3$, the number of wavelength per link $w = 16$, and spare capacity sharing coefficient $\alpha = 0.5$.

improvement. This is because under low link utilization, the blocking due to the lack of eligible transmitters contributes more to the overall blocking compared to the case where link utilization is high and the blocking due to the lack of link capacity is dominating.

### *B. Impact of Limited Number of Add/Drop Ports*

We also investigate the constraint of limited number of add/drop ports on each node under fully tunable transmitters. Computations were made based on equation (14). Assuming average nodal degree $d_n = 3$, link utilization $\rho = 0.3$, and number of wavelengths per link $w = 16$, we change number of add/drop ports $T_s$. Following the derivation in Section II-C, link wavelength utilization $\rho = 0.3$ leads to add/drop port utilization $\rho_{ad} = 2.17\rho \approx 0.65$ (for add/drop port blocking $P_{ad}$ below 0.1%).

Fig. 7 plots the curves under various hop lengths $H$ ranging from 2 to 6. We see that on each curve there is a threshold point, after which a further increase of add/drop ports does not bring much performance improvement. This is because not all lightpaths incident to a node are added/dropped; rather, a large portion of lightpaths only transit the node. Thus, only a limited number of add/drop ports are required to accommodate all the remaining added/dropped lightpaths. Regarding the impact of average hop length, i.e., network density, we see that with the decrease of hop length $H$ (i.e., decrease of network density), the performance saturating point drifts to a larger value. This implies that a network with higher density requires more add/drop ports to reach a performance saturating point. This observation conforms to the finding in (8). In addition, comparing the curves of SBPP and 1:1, it is found that 1:1 seems to demonstrate an earlier threshold point than SBPP. This again agrees with the prior evaluation based on (8).

Finally, though results are not shown here, using the analytical models, we also evaluated the impact of number of add/drop ports under varying link utilization $\rho$ and number of wavelengths per link $w$. It is found that with the increase of link utilization, the threshold point of number of add/drop ports becomes smaller. This is because high link utilization uses up link capacity, which causes no new connections to be established though there are free add/drop ports still available. Regarding the effect of the number of wavelengths on each link, it seems that the change of this parameter does not bring much variation on the ratio of the threshold number of add/drop ports to the total number of capacity units incident to a node (i.e., threshold add/drop ratio). The ratio is always within the range of 40%-50%. Finally, comparing the threshold points of blocking performance of SBPP and 1:1, similar to the observation in Fig. 7, it is found that 1:1 shows a marginally earlier threshold point than SBPP under varying link utilization and numbers of wavelengths per link.

## IV. Assignment of Wavelength and Add/Drop Ports with Limited Tunability

We expect the above analytical models can provide qualitative predictions on the performance of survivable service provisioning. To verify the effectiveness of the models, simulations were also conducted. We developed an effective heuristic algorithm for add/drop port and wavelength assignments. The well-known *wavelength plane* concept is used to help describe the algorithm. A network with $w$ wavelengths consists of $w$ wavelength planes as shown in Fig. 1. A wavelength plane $i$ is made up of the $i^{th}$ wavelength on all the links in the network, and each edge in the wavelength plane is termed *wavelength link*. Based on this concept, the algorithm to find a pair of eligible working and protection lightpaths for SBPP service provisioning is as follows:

Step 1: (Initial conditions) Check the availability of add/drop ports at the source and destination nodes. If there are no free add/drop ports at all, terminate the search and block the request; otherwise, proceed. If proceeding, the first step is to remove all wavelength links that are already in-use by *working* lightpaths from the set of current wavelength planes for this routing request, and set $k_w = 1$.

Step 2: (Working route search) Remove all the wavelength links that have been reserved as *protection* capacity from the $k_w^{th}$ wavelength plane and employ Dijkstra's algorithm to search for a working route within the $k_w^{th}$ wavelength plane. If found, go to Step 3; otherwise, set $k_w = k_w + 1$, and if $k_w \leq w$, restart Step 2, otherwise, the search is terminated and the request is blocked.

Step 3: (Working path found) Note: We arrive here with a $k_w^{th}$ wavelength plane through which a working shortest route was found feasible. Replace all those wavelength links removed in Step 2 and remove all the wavelength links whose corresponding links traversed by the working route found in Step 2 in all the wavelength planes (for the link-disjointness between working and protection routes), and set $k_p = 1$.

Step 4: (Protection route search) In the $k_p^{th}$ wavelength plane, remove all protecting wavelength links that are not eligible to be shared for the protection of the current working route based on the SBPP protection capacity sharing rule.[4] Set the link cost of a sharable wavelength as a small value $\varepsilon$, and a free wavelength link as $1 + \varepsilon$. Then apply Dijkstra's algorithm to search for a protection route. If found, continue to Step 5; otherwise, set $k_p = k_p + 1$ and go to Step 6.

Step 5: (Check add/drop port tunability) Check if there is a pair of free add/drop ports whose transmitters tunability can

[4]The rule is that protection paths can share spare capacity on their common link(s) as long as their corresponding working paths do not share any common link.

cover the wavelengths ($k_w$ and $k_p$) of working and protection lightpaths at both source and destination nodes. If so, establish the service connection and terminate the searching process; otherwise, $k_p = k_p + 1$ and proceed to Step 6.

Step 6: If $k_p \leq w$, go back to Step 4; otherwise, set $k_w = k_w + 1$. If $k_w \leq w$, go back to Step 2; otherwise, terminate the search and block the request.

The algorithm contains three loops to examine all wavelength-plane combinations for the availability of suitable working and protection wavelengths that fall within the tuning range of a pair of free add/drop ports at the source and destination nodes respectively. Step 1 examines the availability of add/drop ports at source and destination nodes so that the searching process can be terminated right away if it is found that no add/drop ports are left at any one of the end nodes. In Step 4, if a protection capacity unit can be shared by a new service connection, a small value $\varepsilon$ is assigned, so that the searching process tends to select this protection capacity unit and maximizes spare capacity sharing; otherwise, for a non-shareable capacity unit, a unit cost $1+\varepsilon$ is assigned. The computational complexity of the algorithm is $O(w^2T(N^2 + M^2H))$, where $T$ is the number of add/drop ports per node, and $H$ is the average hop length of working and protection lightpaths.[5]

The above algorithm is applicable to all network scenarios including fixed transmitter, partially tunable transmitter, and fully tunable transmitters, as well as the 1:1 service provisioning scheme.

If the transmitters on all add/drop ports are fixed, we can simplify the above algorithm to examine only the wavelength-planes that have same indexes as those of free transmitters on the add/drop ports of source and destination nodes. The simplification can lower the computation complexity to be $O(w(N^2 + M^2H))$.

In the case of fully tunable transmitter, it is not necessary to examine add/drop ports tunability as in Step 5 of the generic algorithm. Rather, we only need to examine whether any free add/drop ports are available at both source and destination nodes. As a result, the searching algorithm can be simplified to have a computation complexity at $O(w^2(N^2 + M^2H))$.

Finally, by simplifying Step 4 (protection route search), the algorithm can be extended for 1:1 service provisioning. Because the 1:1 scheme does not allows spare capacity sharing, in Step 4 a sub-step of checking whether any spare capacity can be shared by a new protection lightpath can be removed.[6] The computation complexity of the algorithm can therefore be reduced. Specifically, for the generic partially tunable transmitter case, the computation complexity reduces to $O(w^2TN^2)$, for the fixed transmitter case, to $O(wN^2)$, and for the fully tunable transmitter case, to $O(w^2N^2)$.

[5]Note that the algorithm is based on the active path first (or two-step) searching principle, which may suffer from "trap topology" under some situations [21]. Some strategies [22] to avoid "trap topology" can thus be adopted.

[6]It would be more efficient to employ Suurballe's shortest path pair algorithm to find a pair of disjoint routes that have a minimum sum of hop lengths [23]. However, for simplicity and for a fair comparison with SBPP that employs the two-step process to search for working and protection routes, we also used the two-step process to search for working and protection routes for 1:1.

## V. Test Networks and Simulation Conditions

Simulations were conducted for survivable service provisioning in three test networks. These networks are 14-node 21-link NSFNET, 21-node 25-link ARPA-2 network and 11-node 26-link COST239 networks, as shown Fig. 8. For test purpose, we assumed there were 16 wavelengths on each link in each of the test networks. We followed the widely adopted (and defensible for comparative study purposes) practice of assuming that the arrival of each lightpath request follows a Poisson distribution with rate of $\lambda$ per second and that each established path has a holding time drawn from a negative exponential distribution with a mean of $1/\mu$. We normalized time by assuming $1/\mu = 1$, so that the traffic load between each node pair can be simply considered in units of Erlang as $\lambda$. Also, we assumed each service request consists of only a single lightpath requirement and each node pair has the *same* Erlang traffic load. As the main measure of performance, the blocking probability is computed based on a total of $10^5$ simulated service requests for each test point. An arrival event is considered of being blocked if either working or protection lightpaths are infeasible in the current network state using the route searching and wavelength assignment algorithm above.

Regarding confidence intervals on the estimation of the blocking probabilities, the lowest blocking probability value was estimated based on more than 600 individual blocking events. All other blocking estimates were based on 1000 or more blocking events. Generally in rare-event simulations, at least eight events are required for a reasonable estimate of the average rate of such events. With these 600 to 1000 individual blocking estimates in these simulations, the confidence intervals on the estimate of the mean are thus small.

In addition, for the test cases with fixed wavelength transmitter, the transmitter wavelengths were evenly assigned across the $w$-wavelength spectrum: given $T$ add/drop ports at an OXC node, if $T < w$, we randomly assigned a different wavelength to each of the add/drop ports. Otherwise, we assigned $\lfloor T/w \rfloor$ add/drop ports to each of the $w$ wavelengths, and for the remaining $T - \lfloor T/w \rfloor \cdot w$ add/drop ports, we randomly assigned a different wavelength to each. Note that because there are in general two or more links incident on any node, the number of add/drop ports on the node can be larger than $w$.

For the partially tunable case, we set the tunable degree $d = 6$, which is equivalent to an average tuning range $\bar{r} \simeq 10$. The central wavelength of each partially tunable transmitter is allocated in the way as described for the wavelengths of fixed transmitters. Note that the numerical value of $d = 6$ by itself is not the significant point. Rather, when $d$ is assigned a value in this study, what is more generally significant is the *relative tuning range* that it represents. In this context $d = 6$ represents on average tunability over $\bar{r}/w = 62.5\%$ of the 16 available wavelengths on each fibre.

## VI. Simulation Results and Discussion

### A. Add/Drop Port Number and Ratio

The previous analytical models have found that a saturating process exists–a further increase of the number of add/drop

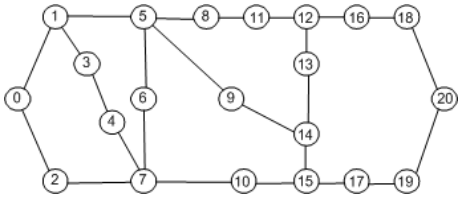


(a) ARPA-2

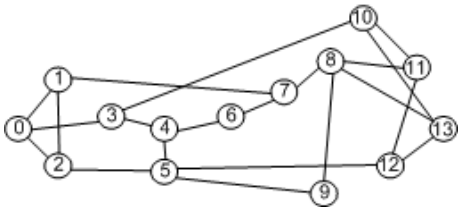


(b) NSFNET

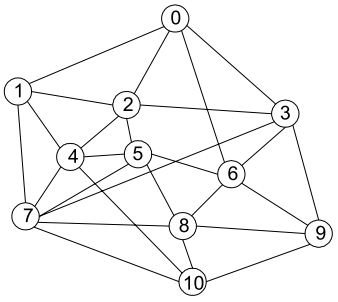


(c) COST239

Fig. 8. Test networks: (a) 21-node 25-link ARPA-2, (b) 14-node 21-link NSFNET, and (c) 11-node 26-link COST239.

ports only marginally improves the service blocking performance when the number of add/drop ports has reached a certain threshold level. In this section, we use simulations to evaluate the impact of the number of add/drop ports on blocking performance in the presence of various extents of transmitter tunability and also verify the *qualitative* effectiveness of the analytical models.

Since the total traffic load originated at each node to all other nodes is assumed to be identical in the simulations (due to the uniform pair-wise traffic assumption), the number of add/drop ports at each node can be meaningfully characterized by a single parameter, $T$. Note that in the case of full tunability, this pool of add/drop ports could be dimensioned directly with an Erlang B full-availability group calculation. However, the limits to tunability and the addition of protection requirements in service provisioning both make the actual dimensioning for low blocking considerably different than a simple Erlang B calculation. By the same reasoning, however, we can expect that $P(B) = ErlangB(T, \lambda)$ will be a lower bound on the achievable blocking in the actual cases considered here.

**Threshold point of number of add/drop ports:** Figs. 9 and 10 show the effects of number of add/drop ports and transmitter tunability on the service blocking performance for SBPP and 1:1 survivable service provisioning respectively. Based on the lower-bounding argument above, reference "Erlang B" curves were computed using Erlang B formula with the total Erlang traffic load and the number of add/drop ports at each node as input. These "Erlang B" curves show what the blocking would be by itself if due only to limited numbers of add/drop ports. Under either fully tunable or fixed wavelength case, we observe a floor in blocking performance emerges, even with continually increasing numbers of add/drop ports. What is happening is that below the threshold of this blocking floor, overall blocking is dominated by the end-node add/drop ports. At the threshold point, blocking becomes limited instead by wavelength-channel continuity and link capacity considerations in the network and *there is no further benefit to provisioning more add/drop ports until either more wavelengths are supported or transmitter tunability increased.* For NSFNET, this threshold is at $T = 14$ (SBPP) and $T = 10$ (1:1) for the fully tunable case and at $T = 16$ (SBPP) and $T = 16$ (1:1) for the fixed transmitter case, which corresponds to 29.2% to 33.3% (SBPP) and 20.8% to 33.3% (1:1) of add/drop ratio at each node. Here the full number of add/drop ports is computed as $T_{full} = d_n w$. Similar observations can be made for the other two test networks.

TABLE II
NUMBERS AND PERCENTAGES OF ADD/DROP PORT THRESHOLD POINTS (SBPP)

| | NSFNET | | COST239 | | ARPA-2 | |
|---|---|---|---|---|---|---|
| | # | % | # | % | # | % |
| **Theoretical** | 14 | 29.2% | 35 | 46.3% | 8 | 21.0% |
| **Fully tunable** | 14 | 29.2% | 32 | 42.3% | 8 | 21.0% |
| **Fixed** | 16 | 33.3% | 48 | 63.5% | 16 | 42.0% |

TABLE III
NUMBERS AND PERCENTAGES OF ADD/DROP PORT THRESHOLD POINTS (1:1)

| | NSFNET | | COST239 | | ARPA-2 | |
|---|---|---|---|---|---|---|
| | # | % | # | % | # | % |
| **Theoretical** | 10 | 20.8% | 21 | 27.8% | 7 | 18.4% |
| **Fully tunable** | 10 | 20.8% | 21 | 27.8% | 7 | 18.4% |
| **Fixed** | 16 | 33.3% | 32 | 42.3% | 16 | 42.0% |

Tables II and III show the threshold numbers of add/drop ports and add/drop ratios for the SBPP and 1:1 schemes respectively. In the tables, the "theoretical" estimations were computed based on the previous analytical models in Section II. Specifically, we determine threshold number of add/drop ports $T$ based on $B(T, \gamma_t d_n w \rho) \leq P_{ad}$. Given $d_n$ and $w$, we need to know $\gamma_t$, $\rho$ and $P_{ad}$. Because there is no real data of $\gamma_t$, $\rho$ and $P_{ad}$, we use simulation data as a substitute for verification purpose. Nonetheless, if real data is provided, then we should directly use it for the computation.

To find $\gamma_t$, we ran a simulation under the assumption of full number of add/drop ports on each node. During the simulation, whenever the $i^{th}$ arrival request was served, we computed the current (the $i^{th}$) network *traffic* add/drop ratio based on (12), i.e., $\gamma_t^i = S_i/(C_w^i + C_p^i)$, where $C_w^i + C_p^i$ was the sum of used working and protection capacity and $S_i$ was the total number of survivable connections being served in the network. After the whole round of simulation (e.g., $10^5$ arrival events were simulated), we averaged all traffic add/drop ratios $\gamma_t^i$ to get an average $\bar{\gamma_t}$.

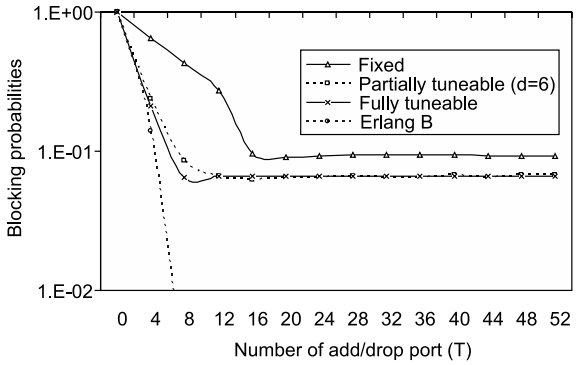


(a) ARPA-2 (0.12 Erlang/node pair)

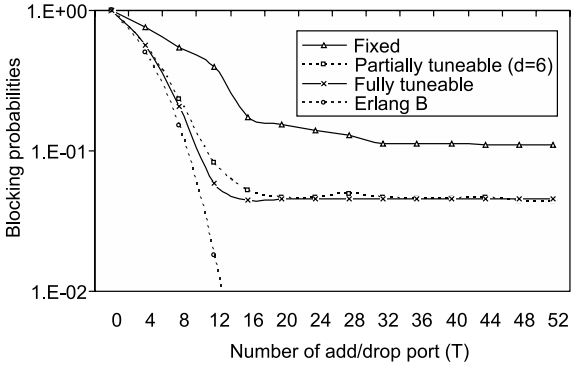


(b) NSFNET (0.5 Erlang/node pair)

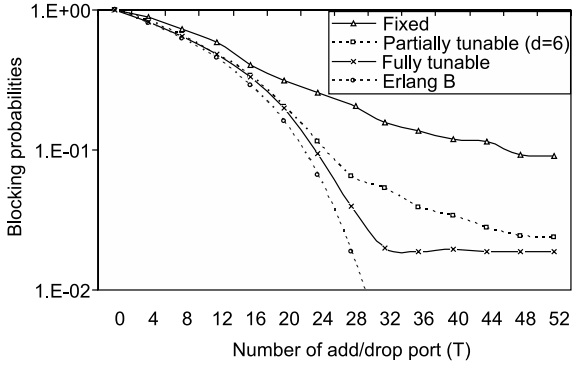


(c) COST239 (2.0 Erlang/node pair)

Fig. 9. SBPP blocking performance versus the number of add/drop ports.

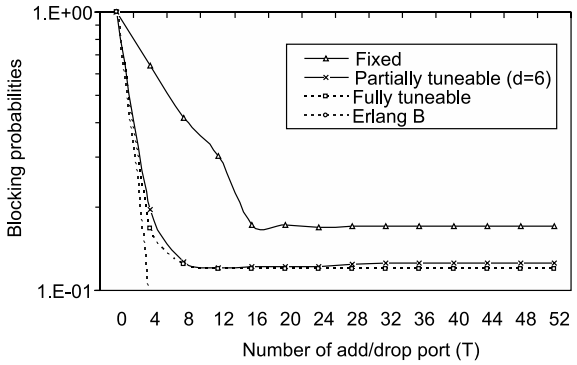


(a) ARPA-2 (0.09 Erlang/node pair)

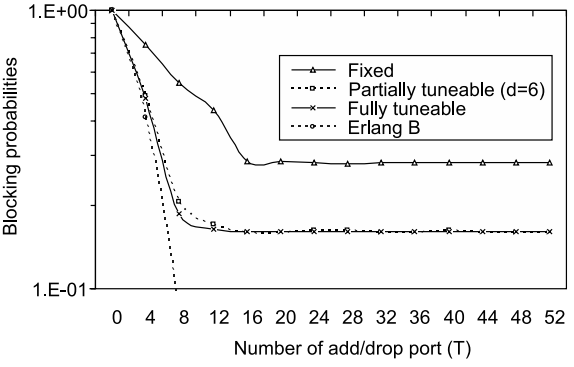


(b) NSFNET (0.4 Erlang/node pair)

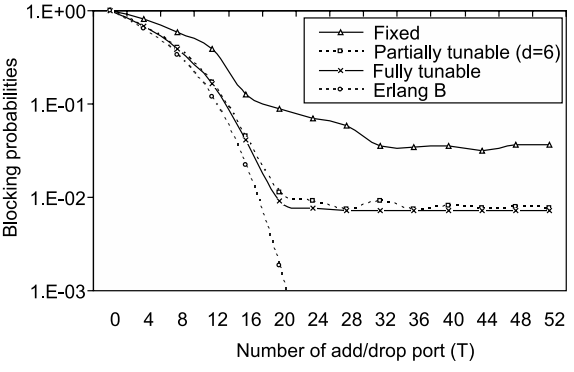


(c) COST239 (1.0 Erlang/node pair)

Fig. 10. 1:1 blocking performance versus the number of add/drop ports.

To identify link utilization $\rho$, we averaged the wavelength utilization (which was further averaged over the whole round of simulation) of each link around an entire network. Mathematically, it is expressed as $\bar{u} = \sum_{i=1}^{M} u_i/M$, where $u_i$ is the wavelength utilization of link $i$ (averaged over the whole round of simulation) and $M$ is the total number of links in the network.

The above simulation also generated a blocking probability, which could be used to set a value for $P_{ad}$. We assumed $P_{ad}$ was one tenth of the blocking probability (under full tunability), such that the blocking from the add/drop ports could be neglected in the overall blocking. For example, in Fig. 9(b) the fully tunable curve has a 0.045 minimum blocking floor, so we set $P_{ad} = 0.0045$.

Finally, based on the above parameters, we found an integer $T$ that satisfied $B(T, \gamma_t d_n w \rho) \leq P_{ad}$, and then computed corresponding $\gamma_s$ using $\gamma_s = T/d_n w$.

By comparing the values obtained based on the theoretical approach and simulations as shown in Tables II and III (compare rows 1 and 2), we find that the analytical model is quite accurate to predict both the threshold numbers of add/drop ports and the threshold add/drop ratios for the fully tunable transmitter case.

**Link utilization:** In association with the blocking performance, we also consider how link utilization can change with the increase of number of add/drop ports for NSFNET. The simulation results are shown in Figs. 11 and 12.[7] The definition and computation approach for the average link

[7]We also obtained similar results for the other two test networks, but do not show them here.

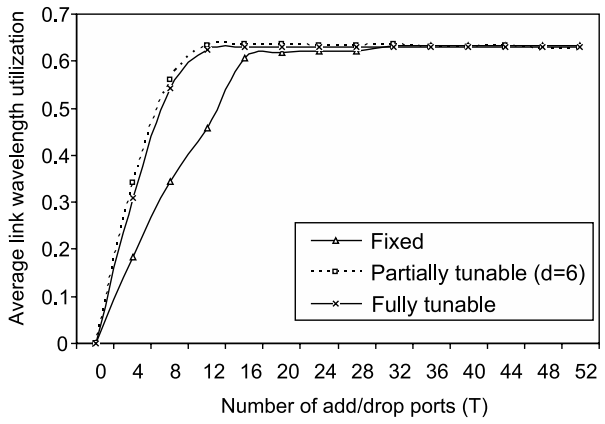


Fig. 11. SBPP average link utilization versus number of add/drop ports; NSFNET (0.5 Erlang/node pair).

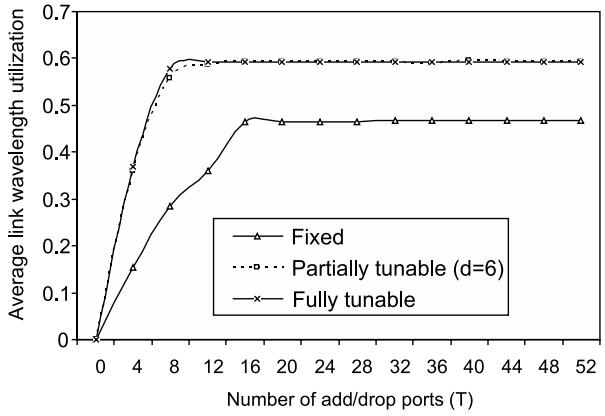


Fig. 12. 1:1 average link utilization versus number of add/drop ports; NSFNET (0.4 Erlang/node pair).

utilization has been described in the previous section as an average over the whole round of simulation and an entire network.

It is found that for both SBPP and 1:1, an increase of the number of add/drop ports helps to improve the average link utilization. This means that sufficient add/drop ports are beneficial to improve network capacity utilization. Also, we see that in each of the curves there is a saturating trend; that is, whenever the number of add/drop ports reaches a specific level, a further increase of the number of add/drop ports does not yield much improvement in link utilization. It is also reasonable to see that these threshold points of the number of add/drop ports have a perfect match to those for blocking probabilities as shown in Figs. 9 and 10.

**Network density:** Tables II and III also show the effect of network density on service provisioning performance. Overall, a network with a higher density needs a relatively larger number of add/drop ports [i.e., a larger system add/drop ratio $T^{threshold}/(d_n w)$] to reach the lowest blocking point (i.e., the blocking floor values in Figs. 9 and 10). Of the test networks here ARPA-2 has the lowest density and requires only 21.0% and 18.4% of full add/drop capability to minimize blocking for SBPP and 1:1, respectively. In contrast, COST239 has the highest density, and needs 42.3% and 27.8% of a full add/drop capability respectively for SBPP and 1:1 to reach the minimum

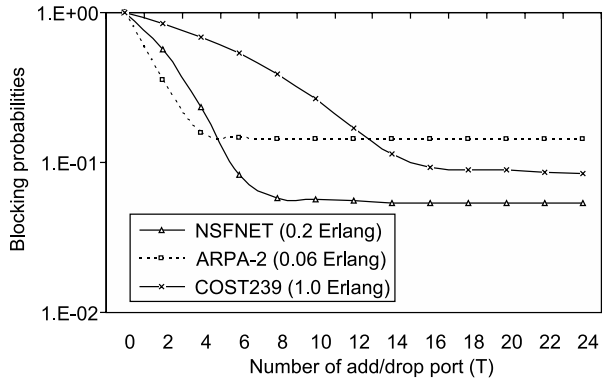


Fig. 13. SBPP blocking performance versus number of add/drop ports. Number of wavelengths on each link $w = 8$.

blocking. Even without tunability the results rank in the same way.

We explain this as an effect purely based on topological considerations. In a network with lower density, relatively more of the flows arriving at any node tend to be transiting lightpaths. Such lightpaths use up two optical line ports on the OXC, but do not require add/drop interfaces at nodes they transit. Thus, in a low-density network, it can be expected that more OXC port capacity will be consumed by through-demands relative to terminating demands. Conversely in a high density network, such as COST239, lightpaths require on average fewer hops from source to destination so the average OXC sees relatively more terminating as opposed to through traffic. As a result, with full tunability ARPA-2 and NSFNET both require less relative add/drop capability to reach minimum blocking than COST239. This therefore again verifies the results obtained from the analytical models shown in Fig. 7, where a longer hop length $H$ shows a smaller threshold point of add/drop port number.

**Number of wavelengths on each link:** We also evaluate the effect of number of wavelengths per link $w$ on the threshold point of add/drop ports. For this, more simulations were conducted to evaluate the blocking performance under link wavelength number $w = 8$. Fig. 13 shows the blocking probability of the fully tunable transmitter case under the SBPP protection scheme. We see that under SBPP, the threshold add/drop ratios are 29.2%, 21.0%, and 42.3% respectively for the NSFNET, ARPA-2, and COST239 networks. These add/drop ratios are exactly the same as those for the networks under link wavelength number $w = 16$. More simulations were also conducted for other network scenarios including the 1:1 scheme and the number of wavelengths on each link $w = 32$. It was found that although under different simulation conditions, the threshold add/drop ratios keep almost the same no matter for the cases of smaller or larger numbers of wavelengths. Thus, it can be concluded that the threshold add/drop ratios seem immune to the change of the number of wavelengths on each link. This observation also agrees with the results obtained in the previous analytical models.

**SBPP versus 1:1:** On the performance difference between SBPP and 1:1, it is obvious that the former can achieve a much better blocking performance than the latter due to its

efficient spare capacity sharing. On the other hand, although both schemes show a saturating trend of blocking performance with the increase of number of add/drop ports, overall 1:1 seems to require a smaller number of add/drop ports to reach a saturating threshold level earlier (See Tables II and III). We see that either under the fully tunable case or the fixed case, 1:1 always shows a smaller add/drop ratio. For example, under the SBPP fully tunable case, NSFNET shows a 29.2% threshold add/drop ratio, while the ratio changes to be smaller, i.e., 20.8%, if the 1:1 protection scheme is used. Similarly, for the fixed transmitter case, COST239 shows a 63.5% threshold add/drop ratio under SBPP, which changes to be 42.3% under 1:1. All these also conform to the observations in Fig. 7.

### *B. Transmitter Tunability*

Let us look at Figs. 9 and 10 again, but now consider the curves of partial tunability. We see that as tuning range increases, the blocking due to wavelength matching considerations between link wavelengths and transmitter wavelengths lowers and the average link utilization increases in each case because transmitters can more efficiently access available wavelength channels. The ultimate blocking floor that arises is due to pure capacity blocking the add/drop ports are available, and all wavelengths are "reachable" but ultimately sheer limits to channel capacity start limiting the achievable blocking. Note, however, that *attainment of this ultimate blocking level requires fewer add/drop ports in all cases with even partial tunability*. Thus, in the presence of partial tunability there is a double benefit because wavelength blocking drops as expected, but one also transitions onto the ultimate capacity-only blocking level sooner, with fewer add/drop ports than required otherwise. Tunability thus not only unlocks capacity from wavelength blocking effects but also makes it fully available with fewer add/drop ports than otherwise required. Significantly, in Figs. 9 and 10 the curves of partial tunability ($d = 6$) are also close to those of full tunability. As might be expected from traffic theoretic principles, this confirms that only partial tunability should really be needed in practice from a network engineering perspective. This thus verifies the observation obtained from the previous analytical models as shown in Fig. 6.

**Network density:** With reference to the asymptotic parts of the curves in Figs. 9 and 10, we can see that a network with higher density apparently benefits more from the transmitter tunability. Under SBPP, COST239 has the highest density and its performance change between the curves of "fixed" and "fully tunable" is the largest. The performance improvement due to the transmitter tunability is about 79%. As the sparest network, ARPA-2 has the smallest performance improvement at about 28%, and finally, for NSFNET that has intermediate density, its performance improvement due to transmitter's full tunability is about 59%. Similar observations can be made for the 1:1 scheme to see that a network with high density can benefit more from transmitter tunability than a network with low density as shown in Fig. 10. All these observations are again in line with the findings in Fig. 6(a), which were obtained based on the analytical models.

**Number of wavelengths on each link:** Fig. 14 shows how the number of wavelengths on each link shows effect on the benefit of transmitter tunability. It is found that for SBPP-based NSFNET when there are eight wavelengths on each link, an around 50% tuning degree ($d/w$) that corresponds to 81.3% tuning rang ($\bar{r}/w$) is required to reach the threshold tuning point. When there are 16 wavelengths on each link, an around 37.5% tuning degree that corresponds to 62.5% tuning range is required to reach the threshold tuning level. Finally, the threshold tuning level for a 32-wavelength case is 31.3% tuning degree and 54.9% tuning range, respectively. We can explain the above findings by "efficiency of trunk group." Under a larger trunk group, i.e., a larger number of wavelengths, even less tunability may suffice to minimize the asymptotic blocking. We also observed this based on the previous analytical models. Thus, this simulation observation again verifies the effectiveness of the analytical models.

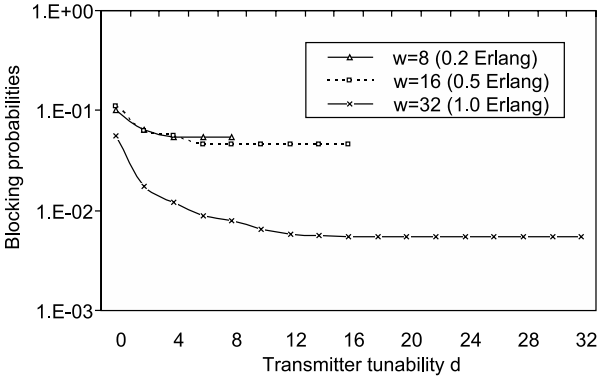


Fig. 14. SBPP blocking performance versus number of wavelengths on each link in NSFNET.

**Link utilization:** Finally, the previous analytical models indicated that at low link utilization, the transmitter tunability can bring more benefit to blocking performance. To verify this, another set of SBPP simulations were conducted for NSFNET under the traffic loads per node pair at 0.4, 0.5, and 0.7 Erlang. The simulation results are shown in Fig. 15. It is found that under a lower network traffic load (i.e., lower link utilization), the transmitter tunability shows a stronger benefit to blocking performance improvement. For example, when the traffic load per node pair is low, 0.4 Erlang, the blocking performance difference between the fixed transmitter case and the fully tunable case is more than 4.6 times; in contrast, when the traffic load per node pair goes high to be 0.7 Erlang per node pair, the benefit of transmitter tunability reduces to be about 1.4 times. Thus, it is confirmed that the previous analytical models make a good qualitative prediction on the relationship between transmitter tunability and link utilization.

## VII. Concluding Comments

We investigated the impacts of limited number of add/drop ports and transmitter tunability on the performance of survivable lightpath service provisioning. We developed analytical models to qualitatively evaluate the impacts. We proposed an effective joint add/drop port and wavelength assignment algorithm for dynamic survivable service provisioning. Computations were made based on the analytical models, and simulations were conducted to evaluate the blocking performance

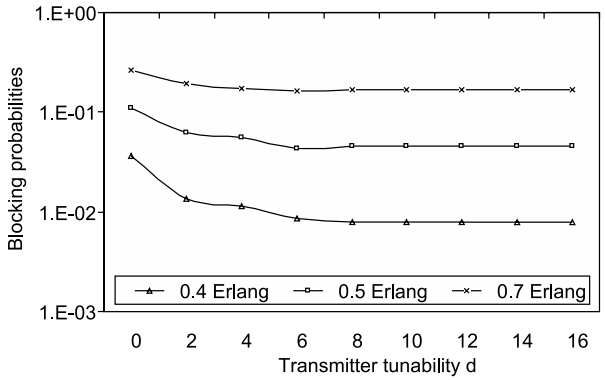


Fig. 15. SBPP blocking performance versus transmitter tunability under full number of add/drop ports and different traffic loads per node pair (i.e., link utilization) in NSFNET.

for SBPP and 1:1. A major finding is that transmitter tunability is a highly "strategic" technology in terms of how it leverages other assets invested in the network, particularly in terms of unlocking access to add/drop ports, and accessibility to the wavelength capacity on fibre links. Following are our detailed research findings:

First, on the number of add/drop ports, we found that there is a saturating trend: before a threshold point of the number of add/drop ports is reached, the increase of add/drop ports can significantly improve network blocking performance. However, after that point, a further increase of the number of add/drop ports does not bring much performance improvement. Moreover, we found that a network with a higher density and/or a lower traffic load requires a larger number of add/drop ports to reach the performance threshold point. However, on the effect of wavelength number on each link, we found that almost no change occurs with the add/drop port threshold point given different wavelength numbers on each link. Thus, it seems that the number of wavelengths on fibre links is not an important factor to affect the add/drop port threshold point. Finally, comparing the performance of SBPP and 1:1, it was found that 1:1 always requires a smaller number of add/drop ports to reach its performance threshold point.

Second, on the effect of transmitter tunability, we found that there is also a saturating process. Before the transmitter tunability increases to a certain level, the blocking performance can be improved fast, but once the tunability reaches a threshold level, a further increase of transmitter tunability does not bring much benefit to performance improvement. Moreover, a network with higher density can have more blocking performance improvement if transmitter tunability changes fixed to fully tunable. In addition, a larger number of wavelengths on each link require a smaller range of transmitter tunability to reach a performance threshold level. Finally, it was also found that the transmitter tunability shows a stronger effect on service provisioning performance in a network with higher traffic load.

We also showed that relatively simple analytical models give a qualitative cross-check and understanding of the effects observed in the simulations such as the saturating trends of add/drop ports and tunability, the effects of network density, etc. The main challenges to obtain even more accurate analytical models are the difficulties in accurately evaluating spare capacity sharing coefficient $\alpha$ and the models for adaptive service routing.

## ACKNOWLEDGMENT

The authors would like to thank the anonymous referees who provided us with many invaluable comments on improving the paper.

This work was substantially conducted while the first author was with the Network Systems group at TRLabs, University of Alberta, in Edmonton, Alberta, Canada.

## REFERENCES

[1] S. Kini, M. Kodialam, T. V. Laksham and, C. Villamizar, "Shared backup label switched path restoration," Internet draft, draft-kini-restoration-shared-backup-00.txt, Aug. 2000.

[2] M. Kodaliam and T. Lakshman, "Dynamic routing of bandwidth guaranteed tunnels with restoration," in *Proc. INFOCOM 2000*, pp. 902-911.

[3] Y. Liu, D. Tipper, and P. Siripongwutikorn, "Approximating optimal spare capacity allocation by successive survivable routing," in *Proc. INFOCOM 2001*, pp. 699-708.

[4] G. Li, D. Wang, C. Kalmanek, and R. Doverspike, "Efficient distributed path selection for shared restoration connections," in *Proc. INFOCOM 2002*, pp. 140-149.

[5] C. Qiao and D. Xu, "Distributed partial information management (DPIM) schemes for survivable networks - part I," in *Proc. INFOCOM 2002*, pp. 302-311.

[6] E. Bouillet, J. F. Labourdette, G. Ellinas, R. Ramamurthy, and S. Chaudhuri, "Stochastic approaches to compute shared mesh restored lightpaths in optical network architectures," in *Proc. INFOCOM 2002*, pp. 801-807.

[7] P. Ho, J. Tapolcai, and H. T. Mouftah, "On optimal diverse routing for shared protection in mesh WDM networks," *IEEE Trans. Reliability*, vol. 53, no. 6, pp. 216-225, June 2004.

[8] C. Ou, J. Zhang, H. Zang, L. Sahasrabuddhe, and B. Mukherjee, "Near-optimal approaches for shared-path protection in WDM mesh networks," in *Proc. IEEE ICC 2003*, pp. 1320-1324.

[9] G. Shen and W. D. Grover, "Survey and performance comparison of dynamic provisioning methods for optical shared backup path protection," in *Proc. 1st GOSP*, Boston, 2005, pp. 387-396.

[10] G. Mohan, C. S. R. Murthy, and A. K. Somani, "Efficient algorithms for routing dependable connections in WDM optical network," *IEEE/ACM Trans. Netw.*, vol. 9, no. 5, pp. 553-566, Oct. 2001.

[11] S. Gowda and K. Sivalingam, "Protection mechanism for optical WDM networks based on wavelength converter multiplexing and backup path relocation techniques," in *Proc. INFOCOM 2003*, pp. 12-21.

[12] P. Ho and H. T. Mouftah, "A novel survivable routing algorithm for segment shared protection in mesh WDM networks with partial wavelength conversion," *IEEE J. Sel. Areas Commun.*, vol. 22, no. 8, pp. 1539-1548, Oct. 2004.

[13] G. Shen, T. H. Cheng, S. K. Bose, *et al.*, "The impact of number of transceivers and their tunabilities on WDM network performance," *IEEE Commun. Lett.*, vol. 4, no. 11, pp 366-368, Nov. 2000.

[14] G. Shen, S. K. Bose, T. H. Cheng, *et al.*, "The impact of the number of add/drop ports in wavelength routing all-optical networks," *Optical Network Mag.*, pp.112-122, Sept./Oct. 2003.

[15] G. Shen and R. S. Tucker, "Translucent optical networks: the way forward," *IEEE Commun. Mag.*, pp.48-54, Feb. 2007.

[16] C. Lee, "Analysis of switching networks," *Bell Systems Technol. J.*, vol. 34, pp.1287-1315, Nov. 1955.

[17] R. Barry and P. Humblet, "Models of blocking probability in all-optical networks with and without wavelength changers," *IEEE J. Sel. Areas Commun.*, vol. 14, no. 5, pp. 858-867, June 1996.

[18] J. Yates, J. Lacey, D. Everitt, and M. Summerfield, "Limited-range wavelength translation in all-optical networks," in *Proc. INFOCOM'96*, pp. 954-961.

[19] G. Shen, S. K. Bose, T. H. Cheng, *et al.*, "Approximate analysis of limited-range wavelength conversion all-optical WDM networks," *Computer Commun.*, vol. 24, pp. 949-957, 2001.

[20] W. D. Grover, *Mesh-Based Survivable Networks: Option and Strategies for Optical, MPLS, SONET, and ATM Networking*. Prentice Hall PTR, 2004.

[21] D. A. Dunn, W. D. Grover, and M. H. MacGregor, "A comparison of k-shortest paths and maximum flow methods for network facility restoration," *IEEE J. Sel. Areas Commun.*, vol. 12, no. 1, pp. 88-99, Jan. 1994.

[22] D. Xu, Y. Xiong, C. Qiao, and G. Li, "Trap avoidance and protection schemes in networks with shared risk link groups," *IEEE J. Lightwave Technol.*, vol. 21, no. 11, pp. 2683-2693, Nov. 2003.

[23] J. W. Suurballe and R. E. Tarjan, "A quick method for finding shortest pairs of disjoint paths," *Networks*, vol. 14, pp. 325-336, 1984.

**Gangxiang Shen** (S'98-M'99) is a Research Fellow with ARC Special Research Center for Ultra-Broadband Information Networks, Department of Electrical Engineering, University of Melbourne, Australia. His research interests are in network survivability, optical networks, and wireless networks. Particularly, his PhD work was focused on *p*-Cycle-based Protected Working Capacity Envelope (PWCE), flow *p*-Cycles, and translucent optical networks, of which the first two have been filed as patents. He has authored and co-authored more than 30 peer-reviewed technical papers.

Dr. Shen received his PhD from Department of Electrical and Computer Engineering, University of Alberta, Canada in January 2006. He received his MSc from Nanyang Technological University in Singapore, and BEng from Zhejiang University in P. R. China. He is a recipient of the Izaak Walton Killam Memorial Scholarship of University of Alberta, the Canadian NSERC Industrial R&D Fellowship, the iCore Graduate Student Scholarship of Alberta, the TRLabs Graduate Student Scholarship, etc.

His personal URL is http://www.buildref.com/home/, and email is g.shen@ee.unimelb.edu.au.

**Wayne D. Grover** (S'74-M'76-SM'90-F'02) received the B.Eng. degree from Carleton University, Canada, the M.Sc. degree from the University of Essex, U.K., and the Ph.D. degree from the University of Alberta, Canada, all in electrical engineering. He had ten years of experience as scientific staff and manager at BNR (now Nortel Networks) working on fiber optics, switching systems, digital radio, and other areas before joining TRLabs as its founding Technical VP in 1986. In this position, he was responsible for the development of the TRLabs' research program and contributed to the development of the TRLabs' sponsorship base; he saw TRLabs through its early growth as a startup to the over-the-100-person level. He now functions as Chief Scientist-Network Systems, TRLabs, and as Professor, Electrical and Computer Engineering, at the University of Alberta. He has authored or co-authored over 200 peer-reviewed publications and has patents issued or pending on nearly 40 topics to date.

Dr. Grover has highly cited key papers in the fields of clock distribution, error-correction coding for fiber optics, digital subscriber loops, and transport network design and survivability mechanisms. He is a recipient of the IEEE Baker Prize Paper Award and IEEE Fellow for his work on survivable and self-organizing networks, as well as the IEEE Canada Outstanding Engineer Award, the Alberta Science and Technology Leadership Award, and the University of Alberta's Martha Cook-Piper Research Award and the prestigious NSERC Steacie Fellowship. He has received TRLabs Technology Commercialization Awards for the licensing of restoration and network-design-related technologies to industry and authored the 2004 book Mesh-based Survivable Networks, Prentice-Hall PTR, and is a co-author of Next Generation Transport Networks: Data, Management and Control Planes, Springer Science, 2005. Current research interests focus on optical network design optimization, new survivability architectures including p-cycles, and new approaches to operation and ongoing re-optimization of dynamic transport networks.